

NATIONAL AERONAUTICAL ESTABLISHMENT
LIBRARY

N. A. E.

R. & M. No. 2679
(10,871)
A.R.C. Technical Report



MINISTRY OF SUPPLY

AERONAUTICAL RESEARCH COUNCIL
REPORTS AND MEMORANDA

Received
17 FEB 1954
LIBRARY

The Influence of Thickness/Chord Ratio on Supersonic Derivatives for Oscillating Aerofoils

By

W. P. JONES, M.A.,

of the Aerodynamics Division, N.P.L.

Crown Copyright Reserved

LONDON : HER MAJESTY'S STATIONERY OFFICE

1954

FIVE SHILLINGS NET

The Influence of Thickness/Chord Ratio on Supersonic Derivatives for Oscillating Aerofoils

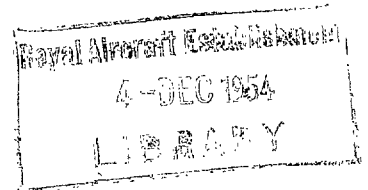
By

W. P. JONES, M.A.,

of the Aerodynamics Division, N.P.L.

*Reports and Memoranda No. 2679**

September, 1947



Summary.—By the use of Temple and Jahn's theory¹ for the oscillating flat plate and Busemann's theory² for aerofoils in steady motion, derivatives are obtained for symmetrical circular-arc and double-wedge aerofoils describing low frequency oscillations at supersonic speeds. It is known that theoretically the torsional aerodynamic damping for a flat plate oscillating about an axis forward of the two-thirds chord position is negative at low frequencies for a limited range of supersonic speeds. In this report, however, it is shown that the effect of increasing thickness/chord ratio is to decrease the range of speeds for which the aerodynamic damping is negative, and for which one degree of freedom flutter is possible. The present theory also allows for the forward movement of the centre of pressure from the half-chord position as the aerofoil thickness is increased, and leads to better estimates of the stiffness derivatives for an actual aerofoil. In practice, the centre of pressure is not at half-chord as predicted by linear theory.

1. *Introductory Remarks.*—Recent experimental values obtained by Bratt³ for the aerodynamic stiffness and damping derivatives of a 7·5 per cent thick symmetrical circular-arc aerofoil tested at supersonic speeds differ widely from the theoretical results of Temple and Jahn¹, and the main object of this theoretical investigation is to find an explanation for the discrepancies. It was thought that the thickness of the aerofoil might be the main cause of the differences between experiment and theory, and so, as a first step, the influence of thickness/chord ratio on the derivatives for low-frequency oscillations is investigated. As shown in Figs. 5 and 6, better agreement between experiment and theory is obtained when this effect is taken into account.

It should be remembered, however, that the given theoretical results are only valid as long as the bow-wave is attached to the leading edge and the flow supersonic everywhere. For the aerofoil tested by Bratt, it becomes detached at about $M_0 = 1·4$ and the flow immediately behind the shock-wave becomes subsonic; the Mach number M_0 being the ratio of the wind speed to the speed of sound. Extrapolated theory, however, indicates, in agreement with experiment, a sharp rise in the damping coefficient as the speed is decreased. It also gives the aerodynamic stiffness derivative to better accuracy than the flat-plate theory.

Busemann's theory² for aerofoils in steady motion is briefly summarised in section 2, and what are believed to be errors in Busemann's third-order coefficients† are pointed out in Appendix I.

No account is taken of boundary-layer effects which are probably responsible for the remaining differences between the theoretical and the experimental results plotted in Figs. 5 and 6.

* Published with the permission of the Director, National Physical Laboratory.

† Since this paper was written, the author has been informed that Laitone⁶ has already given the correct third-order coefficient ($C_3 - D$) for the oblique shock case (see section 2 and Appendix I). In a letter to the *Journal of the Aeronautical Sciences* (August, 1947), Chieh-Chien Chang gives the same formulae for C_3 and D as those derived independently by the writer.

2. *Steady Motion.*—(a) *Pressure Distributions.*—It has been shown by Busemann² that the pressure at any point of an aerofoil in a supersonic stream can be expressed in terms of the local angle of incidence and the leading-edge angle. Thus, for a symmetrical biconvex aerofoil inclined at an angle of incidence α as shown in Fig. 1,

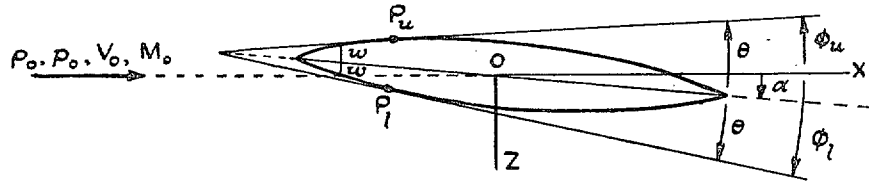


FIG. 1.

the pressure at any point on the upper surface is given to third-order accuracy by

$$\frac{p_u - p_0}{\frac{1}{2}\rho_0 V_0^2} = C_1 \phi_u + C_2 \phi_u^2 + C_3 \phi_u^3 - D w_u^3. \quad \dots \dots \dots (1)$$

Similarly, at any point on the lower surface,

$$\frac{p_l - p_0}{\frac{1}{2}\rho_0 V_0^2} = C_1 \phi_l + C_2 \phi_l^2 + C_3 \phi_l^3 - D w_l^3, \quad \dots \dots \dots (2)$$

where C_1 , C_2 , C_3 and D are functions of the Mach number M_0 of the free stream. The angles $\phi_u (= \theta - \alpha)$ and $\phi_l (= \theta + \alpha)$ represent the local angles of incidence to the free stream of speed V_0 , and θ denotes the local inclination of the surface at P_u (or P_l) to the aerofoil chord. At the leading edge, $\theta = w$, and w_l , w_u respectively denote the corresponding values of ϕ_l and ϕ_u , namely, $w_l = w + \alpha$, and $w_u = w - \alpha$. The terms $D w_u^3$ and $D w_l^3$ give the effect of the shock-waves each side of the leading edge of the aerofoil, but, when the incidence is increased until $\alpha > w$, w_u becomes negative and the flow over the upper surface becomes expansive. The pressure on the upper surface is then given by equation (1) with the $D w_u^3$ term omitted. Since the pressure change due to the presence of a shock-wave is constant everywhere over the aerofoil's surface, it cannot affect the aerodynamic moment about its half-chord axis.

The coefficients C_1 , C_2 , C_3 , D are defined as follows:—

$$\begin{aligned} C_1 &= \frac{2}{\sqrt{(M_0^2 - 1)}}, \\ C_2 &= \frac{1}{2} \frac{[\gamma M_0^4 + (M_0^2 - 2)^2]}{(M_0^2 - 1)^2}, \\ C_3 &= \frac{(\gamma + 1)M_0^8 + (2\gamma^2 - 7\gamma - 5)M_0^6 + 10(\gamma + 1)M_0^4 - 12M_0^2 + 8}{6(M_0^2 - 1)^{7/2}}, \\ D &= \frac{(\gamma + 1)M_0^4}{48(M_0^2 - 1)^{7/2}} [(5 - 3\gamma)M_0^4 + 4(\gamma - 3)M_0^2 + 8], \end{aligned} \quad \dots \dots \dots (3)$$

and they are tabulated for a range of M_0 values in Table 1; $\gamma = 1.4$ being assumed. It should be noted that in equation (3) the expressions for C_3 and D differ from those given by Busemann², which are believed to be in error. The derivation of the coefficients is discussed in some detail in Appendix I.

For some aerodynamic problems, it may be more convenient to express equations (1) and (2) in the form

$$\frac{p - p_0}{\frac{1}{2}\rho_0 V_0^2} = C_1(W/V_0) + C_2(W/V_0)^2 + \left(C_3 - \frac{C_1}{3}\right)(W/V_0)^3 - D(W_e/V_0)^3 \quad \dots \quad (4)$$

where $W = V_0 \tan \phi$ represents the local vertical component of velocity and W_e denotes the component at the leading edge.

(b) *Aerodynamic Forces*.—To illustrate the use of formulae (1) and (2), expressions for the force coefficients for an aerofoil with circular-arc surfaces of equal curvature are derived (see Fig. 1). Let R be the radius of curvature, c the chord, and k the thickness/chord ratio. It then follows that

$$R = \frac{c}{4k} (1 + k^2),$$

and $\tan w = 2k/(1 - k^2)$. It is supposed that the aerofoil incidence α is less than the semi-wedge angle w .

The aerodynamic forces are defined as follows:—

$$\left. \begin{aligned} \text{Lift} &= \int_{-w}^w [(\phi_l - \phi_0) \cos \phi_l - (\phi_u - \phi_0) \cos \phi_u] R d\theta, \\ \text{Drag} &= \int_{-w}^w [(\phi_l - \phi_0) \sin \phi_l + (\phi_u - \phi_0) \sin \phi_u] R d\theta. \end{aligned} \right\} \dots \dots \dots (5)$$

The pitching moment M about an axis at a distance hc behind the leading edge is given by

$$M = Rc \int_{-w}^w (\phi_l - \phi_u) \left(h - \frac{1}{2} + \frac{1 - k^2}{4k} \tan \theta \right) \cos \theta d\theta \quad \dots \dots \dots (6)$$

where ϕ_l and ϕ_u are given by equations (1) and (2) with the D terms included. From equations (3), (5), and (6), it follows that

$$\left. \begin{aligned} C_L &= 2\alpha \left[C_1 \left(1 + \frac{w^2}{6} \right) + \left(C_3 - \frac{C_1}{2} \right) (w^2 + \alpha^2) - D(3w^2 + \alpha^2) \right], \\ C_D &= 2 \left[C_1 \left(1 + \frac{w^2}{6} \right) \left(\alpha^2 + \frac{w^2}{3} \right) + \left(C_3 - \frac{C_1}{6} \right) \left(\frac{w^4}{5} + 2\alpha^2 w^2 + \alpha^4 \right) - D(3w^2 \alpha^2 + \alpha^4) \right], \\ C_M &= 2\alpha \left[C_2 \frac{w}{3} \left(1 - \frac{4w^2}{15} \right) + \left(h - \frac{1}{2} \right) \left[C_1 + C_3 (w^2 + \alpha^2) - D(3w^2 + \alpha^2) \right] \right]. \end{aligned} \right\} \dots \quad (7)$$

A comparison of the numerical values yielded by the above formulae* and results given by exact theory⁴ is made in Tables 2a and 2b for $M_0 = 1.5, 2.0, 2.5$ and 3.0 , with $\alpha = 1$ deg, $k = 0.075$ for a range of h values.

The accuracy of the formulae is slightly better when the C_3 and D terms are included.

* Similar formulae for more general aerofoil sections have been given by Lock⁶.

The pressure on a wedge of infinite chord placed in a supersonic stream is known exactly⁴. In Table 3, a comparison is made between the exact results and those given by formula (1) for wedge semi-angles of 5 deg and 10 deg. For such cases $\phi_u = w_u = w$.

3. *Unsteady Motion.*—(a) *Flat Plate Theory.*—In R. & M. 2140¹ Temple and Jahn derive a solution for the problem of the oscillating plate which is based on linearisation of the equations of motion. The velocity potential ϕ corresponding to the assigned boundary conditions is first determined and then the pressure change $p(x)$ due to the motion is derived from the formula

$$p(x) = \pm \rho_0 \left(\frac{\partial \phi}{\partial t} + V_0 \frac{\partial \phi}{\partial x} \right) \quad \dots \quad \dots \quad \dots \quad \dots \quad (8)$$

As the motion is simple harmonic, let $\phi \equiv \phi' e^{i\omega t}$,

and $p \equiv p' e^{i\omega t}$. Then if $\lambda \equiv \omega c / V_0$ and $x = cX$, formula (8) gives

$$p'(X) = \pm \frac{\rho_0 V_0}{c} \left(i\lambda \phi' + \frac{\partial \phi'}{\partial X} \right) \quad \dots \quad \dots \quad \dots \quad \dots \quad (9)$$

according as points below or above the surface are considered (see Fig. 2). The amplitude of the velocity potential is expressed as an integral involving the Bessel Function J_0 , namely,

$$\phi'(X) = + c \tan \mu_0 \int_0^X e^{-ir\lambda \sec^2 \mu_0} J_0(r\lambda \sec^2 \mu_0 \sin \mu_0) W'(X-r) dr,$$

where $W'(X)$ is the assigned amplitude of the downwash distribution over the chord, and where μ_0 is the Mach angle defined by $\sin \mu_0 = 1/M_0$.

Next suppose that $\lambda \rightarrow 0$. Then, to first order in λ , $J_0 \rightarrow 1$ and

$$\phi'(X) = c \tan \mu_0 \int_0^X (1 - i\lambda \sec^2 \mu_0 \cdot r) W'(X-r) dr. \quad \dots \quad \dots \quad \dots \quad (11)$$

On substitution in equation (9), it follows that

$$p'(X) = \rho_0 V_0 \tan \mu_0 \left(W'(X) - i\lambda \tan^2 \mu_0 \int_0^X W'(\xi) d\xi \right) \quad \dots \quad \dots \quad \dots \quad (12)$$

for points on the lower surface. Since $\tan \mu_0 = C_1/2$, and $\lambda = \omega c / V_0$, the actual pressure change can be expressed in the form

$$p(X) = \frac{1}{2} \rho_0 V_0 C_1 \left[W(X, t) - \tan^2 \mu_0 \int_0^X \frac{c}{V_0} \frac{\partial W(\xi, t)}{\partial t} d\xi \right], \quad \dots \quad \dots \quad \dots \quad (13)$$

where $W(X, t) = W'(X) e^{i\omega t}$ for the case considered. Formula (13) corresponds to the steady motion formula (4) with second and third-order terms omitted. This immediately suggests that the pressure change due to slow variations in W with time would be given to greater accuracy by

$$\frac{p(X)}{\frac{1}{2} \rho_0 V_0^2} = C_1 \left(\frac{\bar{W}}{V_0} \right) + C_2 \left(\frac{\bar{W}}{V_0} \right)^2 + \left(C_3 - \frac{C_1}{3} \right) \left(\frac{\bar{W}}{V_0} \right)^3 - D \left(\frac{\bar{W}_c}{V_0} \right)^3, \quad \dots \quad \dots \quad (14)$$

where

$$\bar{W}(X, t) \equiv W(X, t) - \tan^2 \mu_0 \int_0^X \frac{c}{V_0} \frac{\partial W(\xi, t)}{\partial t} d\xi \quad \dots \quad \dots \quad \dots \quad \dots \quad (15)$$

is regarded as the modified effective vertical component of velocity at the point X at time t . The integral in equation (15) allows for the effect of the motion of the aerofoil profile forward of the point X .

A flat plate describing simple harmonic pitching and translational oscillations with displacements α and z respectively as indicated in the following diagram will have

$$W = V_0 \left(\alpha + \frac{\dot{z}}{V_0} + \frac{c(X-h)\dot{\alpha}}{V_0} \right) \dots \dots \dots (16)$$

where $\dot{\alpha} \equiv \partial\alpha/\partial t$ and $\dot{z} \equiv \partial z/\partial t$.

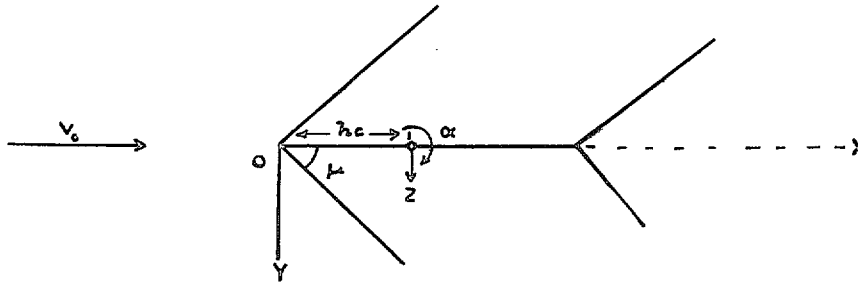


FIG. 2.

The modified effective downwash is then derived by the use of equation (15), and is defined by

$$\bar{W} = V_0 \left[\alpha + \frac{\dot{z}}{V_0} + \frac{c}{V_0} (X - h - X \tan^2 \mu_0) \dot{\alpha} \right] \dots \dots \dots (18)$$

For the lower surface, the pressure distribution is given by formula (14), where \bar{W}/V_0 is defined by formula (18), and where \bar{W}_e is the value of \bar{W} at the lower side of the leading edge. For the upper surface, the flow is expansive; the values of \bar{W} are regarded as negative; and as there is no shock the D term is omitted. Hence, for a flat plate, the lift distribution $l(X)$ is given by

$$\frac{l(X)}{\rho_0 V_0^2} = C_1 \left(\frac{\bar{W}}{V_0} \right) + \left(C_3 - \frac{C_1}{3} \right) \left(\frac{\bar{W}}{V_0} \right)^3 - \frac{D}{2} \left(\frac{\bar{W}_e}{V_0} \right)^3 \dots \dots \dots (19)$$

If the first term only is retained, equation (19) yields limiting values for the fundamental derivative coefficients which agree with those given by Temple and Jahn¹ as will be shown in the next section.

(b) *Thick Aerofoil Theory*.—Consider next the aerodynamic forces on a symmetrical circular-arc aerofoil in unsteady motion.

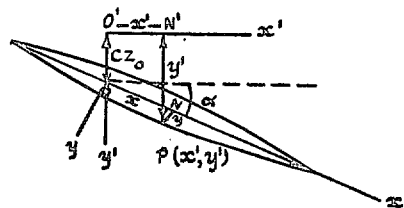


FIG. 3.

Let the reference point O be displaced a distance cz_0 relative to its initial position O', and let α represent the angular displacement about O at time t . At the point P, the velocity component perpendicular to the direction of flow of the free stream is

$$W = \frac{\partial z}{\partial t} + V_0 \frac{\partial z}{\partial x'}, \quad \dots \quad (20)$$

where $z = cz_0 + x \sin \alpha + y \cos \alpha$. On differentiation, equation (20) yields

$$W = c\dot{z}_0 + V_0 \tan(\theta + \alpha) + x'\dot{\alpha}, \quad \dots \quad (21)$$

where $\dot{z}_0 \equiv \partial z_0 / \partial t$, $\dot{\alpha} \equiv \partial \alpha / \partial t$, and $x' = x \cos \alpha - y \sin \alpha$. If the rates of change of \dot{z}_0 and $\dot{\alpha}$ are slow, and if θ and α are small; then, to second-order accuracy, the vertical component of velocity at P is

$$\frac{W}{V_0} = \frac{c\dot{z}_0}{V_0} + \theta + \alpha + \frac{c(X-h)\dot{\alpha}}{V_0} \quad \dots \quad (22)$$

where $cX = hc + x'$ represents the distance along the chord referred to the leading edge as origin. The modified effective vertical component \bar{W} for points on the lower surface of the aerofoil is given by equation (15) as

$$\frac{\bar{W}_l}{V_0} = \theta(X) + \alpha + \frac{c\dot{z}_0}{V_0} + \frac{c\dot{\alpha}}{V_0} (X - h - X \tan^2 \mu_0), \quad \dots \quad (23)$$

and for the upper surface

$$\frac{\bar{W}_u}{V_0} = \theta(X) - \alpha - \frac{c\dot{z}_0}{V_0} - \frac{c\dot{\alpha}}{V_0} (X - h - X \tan^2 \mu_0). \quad \dots \quad (24)$$

At the leading edge, $\theta = w$ and $X = 0$, and equations (23) and (24) yield

$$\bar{W}_e = V_0 \left(w \mp \alpha \mp \frac{c\dot{z}_0}{V_0} \mp \frac{hc\dot{\alpha}}{V_0} \right), \quad \dots \quad (25)$$

the upper and lower signs corresponding to the upper and lower surfaces of the aerofoil respectively. The pressure changes on the surfaces can then be derived by the substitution of the appropriate values of \bar{W} , as given by equations (23), (24), and (25), in equation (14). The aerodynamic forces and moments are given by equations (5) and (6), when the substitutions $\phi_l = \theta + \alpha$, and $\phi_u = \theta - \alpha$ are made.

For a symmetrical circular-arc aerofoil, the profile is defined to second-order accuracy in the thickness/chord ratio k by

$$y = 2kc(X - X^2), \quad \dots \quad (26)$$

and the variation in incidence is given by

$$\theta = 4k\left(\frac{1}{2} - X\right) \quad \dots \quad (27)$$

with $\theta = w = 2k$ at the leading edge.

Let the lift L and moment M about a reference axis at hc behind the leading edge be expressed in the form

$$\begin{aligned}\frac{L}{\rho_0 c V_0^2} &= l_z z_0 + l_z \left(\frac{c \dot{z}_0}{V_0} \right) + l_\alpha \alpha + l_a \left(\frac{c \dot{\alpha}}{V_0} \right), \\ \frac{M}{\rho_0 c^2 V_0^2} &= m_z z_0 + m_z \left(\frac{c \dot{z}_0}{V_0} \right) + m_\alpha \alpha + m_a \left(\frac{c \dot{\alpha}}{V_0} \right)\end{aligned}\quad \dots \quad \dots \quad \dots \quad (28)$$

where the actual translational displacement is cz_0 and α represents the angular displacement. Then, to second-order accuracy in the displacements and the thickness/chord ratio, it follows from equations (5) and (6) that

$$\begin{aligned}L &= c \int_0^1 (p_l - p_u) dX, \\ M &= -c^2 \int_0^1 (p_l - p_u)(X - h) dX.\end{aligned}\quad \dots \quad \dots \quad \dots \quad (29)$$

If $t_0 \equiv \tan \mu_0$, equations (14), (23) and (24) yield

$$\frac{p_l - p_u}{\frac{1}{2} \rho_0 V_0^2} = 2 \left[\alpha + \frac{c \dot{z}_0}{V_0} + \frac{c \dot{\alpha}}{V_0} (X - h - X t_0^2) \right] [C_1 + 2C_2 \theta]. \quad \dots \quad \dots \quad (30)$$

By the use of equations (29) and (30) the following set of fundamental derivatives is derived for symmetrical circular-arc profiles of thickness/chord ratio k :—

$$\begin{aligned}l_z &= 0, \quad l_z = C_1, \quad m_z = 0, \quad m_z = -C_1 \left(\frac{1}{2} - h \right) + \frac{2}{3} C_2 k, \\ l_\alpha &= C_1, \quad l_\alpha = C_1 \left(\frac{1 - t_0^2}{2} - h \right) - \frac{2}{3} (1 - t_0^2) k C_2, \\ m_\alpha &= -C_1 \left(\frac{1}{2} - h \right) + \frac{2}{3} C_2 k, \\ m_a &= -C_1 \left[\frac{1}{3} - h + h^2 - t_0^2 \left(\frac{1}{3} - \frac{h}{2} \right) \right] + \frac{4k}{3} C_2 \left[\frac{1}{2} - h - \frac{t_0^2}{2} (1 - h) \right].\end{aligned}\quad \dots \quad \dots \quad (31)$$

Curves of m_α and m_a with k and h varied are given in Figs. 5 and 6.

For a symmetrical double-wedge of thickness/chord ratio k , the appropriate formulae are:—

$$\begin{aligned}l_z &= 0, \quad l_z = C_1, \quad m_z = 0, \quad m_z = -C_1 \left(\frac{1}{2} - h \right) + \frac{C_2 k}{2}, \\ l_\alpha &= C_1, \quad l_\alpha = C_1 \left(\frac{1 - t_0^2}{2} - h \right) - \frac{k C_2}{2} (1 - t_0^2), \\ m_\alpha &= -C_1 \left(\frac{1}{2} - h \right) + \frac{C_2 k}{2}, \\ m_a &= -C_1 \left[\frac{1}{3} - h + h^2 - t_0^2 \left(\frac{1}{3} - \frac{h}{2} \right) \right] + k C_2 \left[\frac{1}{2} - h - \frac{t_0^2}{2} (1 - h) \right].\end{aligned}\quad \dots \quad \dots \quad (32)$$

A comparison of formulae (31) and (32) shows that the derivatives for a circular-arc profile of thickness/chord ratio h are equal to those for a double-wedge of thickness/chord ratio $4h/3$. Alternatively, a double-wedge of thickness/chord ratio h corresponds to a circular-arc profile of ratio $3h/4$.

Formulae (31) and (32) are the limiting forms of the derivatives when the motion is very slow as for a very low-frequency oscillation. For a flat-plate, $h = 0$, and formulae (31) and (32) then reduce to the limiting values given by the Temple and Jahn theory¹. To allow for frequency parameter variation, the approximations given below could be used for a symmetrical circular-arc profile, namely,

$$\left. \begin{aligned} l_z &= \bar{l}_z, \quad l_z = \bar{l}_z, \quad m_z = \bar{m}_z, \quad m_z = \bar{m}_z + \frac{2}{3}C_2k, \\ l_\alpha &= \bar{l}_\alpha, \quad l_\alpha = \bar{l}_\alpha - \frac{2}{3}(1 - t_0^2)kC_2, \\ m_\alpha &= \bar{m}_\alpha + \frac{2}{3}C_2k, \\ m_\alpha &= \bar{m}_\alpha + \frac{4k}{3}C_2 \left[\frac{1}{2} - h - \frac{t_0^2}{2}(1 - h) \right], \end{aligned} \right\} \dots \dots \dots \dots \dots (33)$$

where $\bar{l}_z, \bar{l}_\alpha$, etc., are the frequency dependent derivatives for a flat plate as given by Temple and Jahn¹. For a double-wedge, the factor h in formulae (33) must be replaced by $3h/4$. It may be that the influence of thickness varies with frequency parameter, but for values of λ near zero, formulae (33) may yield slightly better approximations to the derivatives for a circular-arc profile than those given by formulae (31).

4. *Conclusions.*—The derivative formulae given in section 3(b) correspond to second-order theory and adiabatic conditions, and yield results in better agreement with experiment than those given by the linear flat-plate theory. The stiffness derivatives for zero frequency could be deduced exactly as in Ref. 4 or to third-order accuracy by the use of formulae (1) and (2). It is doubtful, however, whether Busemann's third-order formula used in conjunction with equation (15) would give reliable estimates of the damping for thick aerofoils since the concept of a modified effective normal component of velocity may not be justifiable to this order of accuracy near $M = 1$. For larger values of M , the third-order term has little effect on the final results and can be neglected.

Acknowledgement.—The writer is greatly indebted to Mrs. H. N. Wilkinson, B.Sc., who did most of the numerical work included in this report.

APPENDIX I

Formulae of the Busemann Type

Third-Order Coefficients.—As the third-order coefficients C_3 and D defined in section 2 of this report differ from those given in Busemann's paper², their derivation is discussed here in some detail. The method used follows closely that adopted in Ref. 4 to obtain the second-order coefficients. Busemann only gives the final formulae in his report, and he does not state clearly how they were derived.

Consider the case of supersonic flow past a curved surface inclined at an angle w to the free stream at its leading edge as shown in Fig. 4 below.

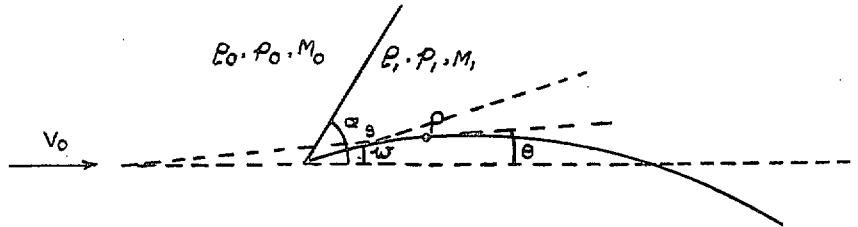


FIG. 4.

Let α_s be the angle between the shock-wave and the direction of flow, and let θ be the local incidence at a point P on the surface. The symbols ρ_0, p_0, M_0 , and ρ_1, p_1, M_1 , represent the density, pressure, and Mach number respectively in front and behind the shock-wave, and ρ, p, M define the local conditions at P. Then, if $X = \rho_1/\rho_0$, as in Ref. 4, it can be shown that

$$X = \frac{\tan \alpha_s}{\tan (\alpha_s - w)}, \quad \dots \dots \dots (34)$$

$$\frac{p_1}{p_0} = \frac{(\gamma + 1)X - \gamma + 1}{\gamma + 1 - (\gamma - 1)X}, \quad \dots \dots \dots (35)$$

$$M_0^2 \sin^2 \alpha_s = \frac{2X}{\gamma + 1 - (\gamma + 1)X}, \quad \dots \dots \dots (36)$$

$$M_1^2 \sin^2 (\alpha_s - w) = \frac{2}{(\gamma + 1)X - \gamma + 1}. \quad \dots \dots \dots (37)$$

These relations define conditions behind the shock-wave for any given w and M_0 . The pressure at any point P on the surface is expressible in terms of the conditions immediately behind the shock-wave by means of the following relations:—

$$\frac{p}{p_1} = \frac{g(\mu)}{g(\mu_1)}, \quad \dots \dots \dots (38)$$

$$w - \theta = f(\mu_1) - f(\mu), \quad \dots \dots \dots (39)$$

where

$$g(\mu) = [\sin^2 \mu / (\gamma - \cos 2\mu)]^{\gamma/(\gamma-1)},$$

$$f(\mu) = \sqrt{\left(\frac{\gamma + 1}{\gamma - 1}\right)} \tan^{-1} \left(\sqrt{\left(\frac{\gamma + 1}{\gamma - 1}\right)} \tan \mu \right) - \mu,$$

and the local Mach angle $\mu = \sin^{-1} 1/M$. By the use of formulae (34) to (39) and the tables given in Ref. 4, the exact pressure distribution can then be calculated.

Approximations to formulae (35) and (38) are obtained by expansion of the various functions involved in ascending power series of the angular deviations. If $t = \tan \alpha_s$, formula (34) gives

$$X = 1 + \left(\frac{1+t^2}{t}\right)w + \left(\frac{1+t^2}{t^2}\right)w^2 + \frac{(1+t^2)(3+t^2)}{3t^3}w^3 + O(w^4) \quad \dots \quad (40)$$

and, by substituting in formula (35), it follows that

$$\begin{aligned} \frac{p_1}{p_0} = 1 + \frac{\gamma(1+t^2)w}{t} \left\{ 1 + \frac{[1-t^2 + \gamma(1+t^2)]w}{2t} \right. \\ \left. + \frac{w^2[3t^4 - 2t^2 + 3 + 6\gamma(1-t^4) + 3\gamma^2(1+t^2)^2]}{12t^2} + \dots \right\} \quad \dots \quad (41) \end{aligned}$$

Let

$$\begin{aligned} a &\equiv \gamma(1+t_0^2) - 1 + t_0^2, \\ b &\equiv \frac{(\gamma+1)(1+t_0^2)^2}{t_0^2} \\ t_0 &\equiv \tan \mu_0 = 1/\sqrt{(M_0^2 - 1)}. \end{aligned}$$

Then, from formulae (34) and (36), it can be deduced that

$$t = t_0 \left[1 + \frac{bt_0 w}{4} + \left(ab + \frac{b^2}{4}\right) \frac{w^2 t_0^2}{8} + \dots \right] \quad \dots \quad (42)$$

Substitution for t in equation (41) immediately yields

$$\frac{p_1 - p_0}{p_0} = \frac{\gamma M_0^2}{2} \left\{ C_1(M_0)w + C_2(M_0)w^2 + [C_3(M_0) - D(M_0)]w^3 \right\}, \quad \dots \quad (43)$$

where

$$\left. \begin{aligned} C_1(M) &= 2/\sqrt{(M^2 - 1)}, \\ C_2(M) &= [\gamma M^4 + (M^2 - 2)^2]/2(M^2 - 1)^2, \\ C_3(M) - D(M) &= \frac{3(\gamma+1)^2 M^8 + 4(3\gamma^2 - 12\gamma - 7)M^6 + 72(\gamma+1)M^4 - 96M^2 + 64}{48(M^2 - 1)^{7/2}} \end{aligned} \right\} \quad (44)$$

Formula (43) gives the pressure increase in passing through the shock.

For adiabatic flow, formula (38) yields on expansion by Taylor's theorem

$$\frac{p - p_1}{p_1} = \frac{1}{g(\mu_1)} \left[(\mu - \mu_1) g'(\mu_1) + \frac{(\mu - \mu_1)^2}{2} g''(\mu_1) + \frac{(\mu - \mu_1)^3}{6} g'''(\mu_1) \right] \quad \dots \quad (45)$$

where $g'(\mu) \equiv \partial g/\partial \mu$, etc. Furthermore, expansion of the right-hand side of formula (39) and inversion of the series obtained yields

$$\mu - \mu_1 = d_1(\theta - w) + d_2(\theta - w)^2 + d_3(\theta - w)^3, \quad \dots \quad (46)$$

where

$$d_1 = \frac{1}{f'}, \quad d_2 = -\frac{1}{2} \frac{f''}{f'^3}$$

$$d_3 = -\frac{f'''}{6f'^4} + \frac{1}{2} \frac{f''^2}{f'^5}$$

and $f' = \partial f/\partial \mu_1$, etc. By the use of formula (37), however, it can be proved that

$$\mu_1 = \mu_0 + \frac{(\gamma + 1)s_0^2 - 2}{2} \left(w + \frac{(\gamma + 1)}{2} s_0^2 t_0 w^2 \right) \quad \dots \quad (47)$$

where $s_0^2 \equiv 1 + t_0^2 = \sec^2 \mu_0$. From equations (45) and (46), it follows that

$$\frac{\dot{p} - \dot{p}_1}{\dot{p}_1} = \frac{\gamma M_1^2}{2} \left[C_1(M_1)(\theta - w) + C_2(M_1)(\theta - w)^2 + C_3(M_1)(\theta - w)^3 \right], \quad \dots \quad (48)$$

where C_1 and C_2 are as defined by formulae (44) and

$$C_3(M) = \frac{(\gamma + 1)M^8 + (2\gamma^2 - 7\gamma - 5)M^6 + 10(\gamma + 1)M^4 - 12M^2 + 8}{6(M^2 - 1)^{7/2}}. \quad \dots \quad (49)$$

Now formula (43) gives \dot{p}_1/\dot{p}_0 and formula (48) gives \dot{p}/\dot{p}_1 , and hence by multiplication the formula for \dot{p}/\dot{p}_0 can be deduced. By the use of formula (47), the coefficients $C_1(M_1)$, etc., of formula (48) are expressed in terms of M_0 or μ_0 , and after considerable reduction a formula for \dot{p}/\dot{p}_0 is derived, namely,

$$\frac{\dot{p}}{\dot{p}_0} = 1 + \frac{\gamma M_0^2}{2} \left[C_1(M_0)\theta + C_2(M_0)\theta^2 + C_3(M_0)\theta^3 - D(M_0)w^3 \right]. \quad \dots \quad (50)$$

This formula must correspond to (43) when $\theta = w$, hence it follows that

$$D(M) = \frac{(\gamma + 1)M^4}{48(M^2 - 1)^{7/2}} \left[(5 - 3\gamma)M^4 + 4(\gamma - 3)M^2 + 8 \right]. \quad \dots \quad (51)$$

In Ref. 2, Busemann gives

$$C_3 = \left\{ \frac{(\gamma + 1)M^4}{4} \left(M^2 - \frac{5 + 7\gamma - 2\gamma^2}{2(\gamma + 1)} \right)^2 + \frac{3}{4} \left(M^2 - \frac{4}{3} \right)^2 \right. \\ \left. + M^4 \frac{(-4\gamma^4 + 28\gamma^3 + 11\gamma^2 - 8\gamma - 3)}{24(\gamma + 1)} \right\} / (M^2 - 1)^{7/2}, \quad \dots \quad (52)$$

$$D = \frac{(\gamma + 1)M^4}{12} \left[\frac{5 - 3\gamma}{4} \left(M^2 - \frac{6 - 2\gamma}{5 - 3\gamma} \right)^2 - \frac{\gamma^2 + 1}{5 - 3\gamma} \right] / (M^2 - 1)^{7/2}. \quad \dots \quad (53)$$

If the first term in formula (52) is divided by 6 instead of 4, and if $\gamma^2 + 1$ is replaced by $\gamma^2 - 1$ in the last term of formula (53), then the above expressions can be reduced to the formulae given in this report.

REFERENCES

<i>No.</i>	<i>Author</i>	<i>Title, etc.</i>
1	G. Temple and H. A. Jahn	Flutter at Supersonic Speeds. Derivative Coefficients for a Thin Aerofoil at Zero Incidence. R. & M. 2140. April, 1945.
2	A. Busemann	Aerodynamic Lift at Supersonic Speeds. (Lecture given at the 5th Volta Conference at Rome). (<i>L.F.F.</i> , Vol. 12, No. 6, 3.10.35). Translated by W. J. Stern, A.R.C.S. Communicated by D.S.R. Air Ministry. A.R.C. 2844.
3	J. B. Bratt and A. Chinneck	Measurements of Mid-chord Pitching Moment Derivatives at High Speeds. R. & M. 2680. July, 1947.
4	Edmonson, Murnaghan and Snow	The Theory and Practice of Two-dimensional Supersonic Pressure Calculations. Johns Hopkins University, Bumble Bee Report No. 26, 1945.
5	C. N. H. Lock	Examples of the Application of Busemann's Formula to Evaluate the Aerodynamic Force Coefficients on Supersonic Aerofoils. R. & M. 2101. September, 1944.
6	E. V. Laitone	Exact and Approximate Solutions of Two-Dimensional Oblique Shock Flow. <i>Jour. Aero. Sci.</i> January, 1947.

TABLE 1

Values of C_1 , C_2 , C_3 and D $\gamma = 1.4$

Mach number	C_1	C_2	C_3	D
1.10	4.364	30.32	568.9	24.53
1.12	3.965	21.32	304.7	11.66
1.14	3.654	15.91	180.0	5.927
1.16	3.402	12.40	114.4	3.120
1.18	3.193	10.01	76.97	1.639
1.20	3.015	8.307	54.00	0.8121
1.22	2.862	7.049	39.32	0.3351
1.24	2.728	6.096	29.46	0.05256
1.26	2.609	5.357	22.68	-0.1169
1.28	2.503	4.771	17.81	-0.2184
1.30	2.408	4.300	14.25	-0.2780
1.32	2.321	3.916	11.59	-0.3111
1.34	2.242	3.598	9.571	-0.3276
1.36	2.170	3.333	8.005	-0.3330
1.38	2.103	3.109	6.776	-0.3316
1.40	2.041	2.919	5.801	-0.3258
1.42	1.984	2.755	5.019	-0.3175
1.44	1.930	2.614	4.375	-0.3069
1.46	1.880	2.491	3.852	-0.2958
1.48	1.833	2.383	3.419	-0.2839
1.50	1.789	2.288	3.059	-0.2725
1.60	1.601	1.949	1.938	-0.2171
1.70	1.455	1.748	1.410	-0.1715
1.80	1.336	1.618	1.145	-0.1354
1.90	1.238	1.529	1.005	-0.1062
2.0	1.155	1.467	0.9343	-0.08214
2.5	0.8730	1.320	0.9428	-0.00442
3.0	0.7072	1.269	1.112	0.04251
3.5	0.5963	1.245	1.310	0.07805
4.0	0.5164	1.232	1.513	0.1081
∞	0	1.200	∞	∞

TABLE 2a

Values of C_M $\alpha = 1 \text{ deg}; k = 0.075$

h	$M_0 = 1.5$			$M_0 = 2.0$		
	Second-order approximation	Third-order approximation	Exact	Second-order approximation	Third-order approximation	Exact
0.5	0.00398	0.00398	0.00461	0.00255	0.00255	0.00254
0.4	-0.00228	-0.00259	-0.00207	-0.00149	-0.00158	-0.00164
0.3	-0.00853	-0.00915	-0.00875	-0.00553	-0.00572	-0.00587
0.2	-0.0148	-0.0157	-0.0154	-0.00957	-0.00985	-0.01002
0.1	-0.0210	-0.0223	-0.0221	-0.0136	-0.0140	-0.0142
0	-0.0273	-0.0288	-0.0288	-0.0176	-0.0181	-0.0184

h	$M_0 = 2.5$			$M_0 = 3.0$		
	Second-order approximation	Third-order approximation	Exact	Second-order approximation	Third-order approximation	Exact
0.5	0.00230	0.00230	0.00225	0.00221	0.00221	0.00215
0.4	-0.000757	-0.000833	-0.000890	-0.000266	-0.000345	-0.000419
0.3	-0.00381	-0.00396	-0.00405	-0.00274	-0.00290	-0.00299
0.2	-0.00686	-0.00709	-0.00719	-0.00521	-0.00545	-0.00555
0.1	-0.00991	-0.01022	-0.01033	-0.00768	-0.00800	-0.00813
0	-0.01296	-0.01334	-0.01347	-0.01015	-0.01055	-0.01072

TABLE 2b

Values of C_L and C_D $\alpha = 1 \text{ deg}; k = 0.075$

M_0	C_L			C_D		
	Second-order approximation	Third-order approximation	Exact	Second-order approximation	Third-order approximation	Exact
1.5	0.0628	0.0652	0.0663	0.0280	0.0287	0.0288
2.0	0.0405	0.0410	0.0416	0.0181	0.0183	0.0182
2.5	0.0306	0.0310	0.0312	0.0137	0.0139	0.0138
3.0	0.0248	0.0253	0.0255	0.0111	0.0113	0.0112

TABLE 3

Values of p_1/p_0 for a Wedge of Angle $2w$

M_0	$w = 5 \text{ deg}$			M_0	$w = 10 \text{ deg}$		
	Second-order approximation	Third-order* approximation	Exact		Second-order approximation	Third-order approximation	Exact
1.1	1.518	1.825	No value	1.1	2.428	4.883	No value
1.2	1.329	1.365	No value	1.2	1.786	2.071	No value
1.24	1.306	1.327 (1.336)†	1.417	1.3	1.652	1.744	No value
1.26	1.298	1.315	1.347	1.4	1.611	1.656	No value
1.3	1.287	1.299	1.312	1.42	1.608	1.648 (1.662)	1.830
1.4	1.275	1.281	1.284	1.46	1.603	1.636	1.697
1.5	1.273	1.277	1.278	1.5	1.602	1.630	1.667
1.6	1.277	1.280	1.281	1.6	1.607	1.628	1.644
1.7	1.284	1.286	1.286	1.7	1.622	1.639	1.647
1.8	1.293	1.294	1.295	1.8	1.641	1.656	1.662
1.9	1.302	1.305	1.304	1.9	1.664	1.679	1.682
2.0	1.314	1.316 (1.316)	1.316	2.0	1.690	1.705 (1.711)	1.707
2.5	1.378	1.380	1.380	2.5	1.843	1.865	1.864
3.0	1.450	1.454	1.453	3.0	2.022	2.058	2.053
3.5	1.527	1.535	1.534	3.5	2.219	2.274	2.270
4.0	1.610	1.620 (1.626)	1.619	4.0	2.430	2.514 (2.559)	2.508

* $\gamma = 1.4$ assumed.

† Values given by Busemann's formula are shown in brackets.

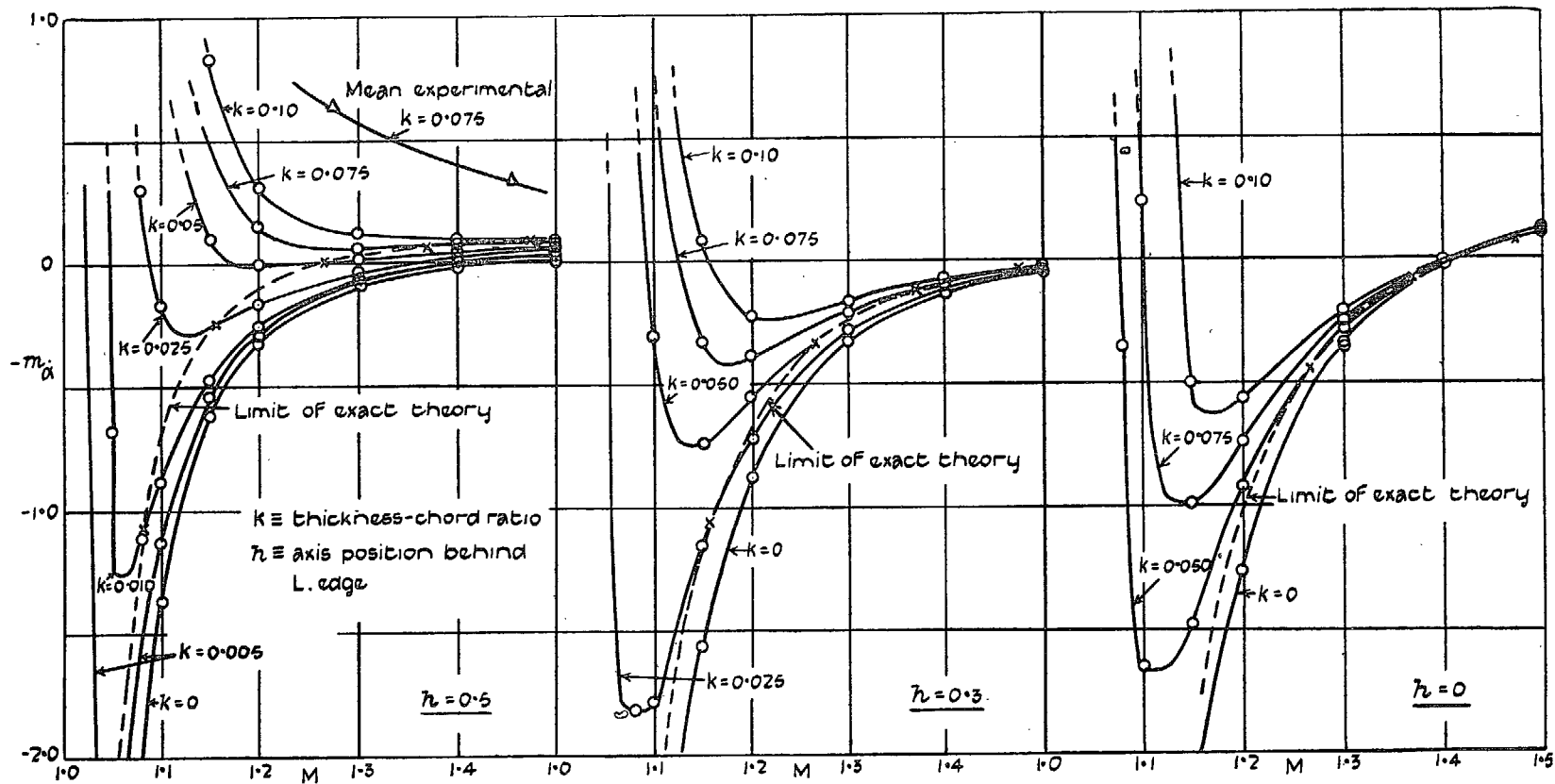


FIG. 5. Influence of thickness/chord ratio on the torsional aerodynamic damping coefficient.

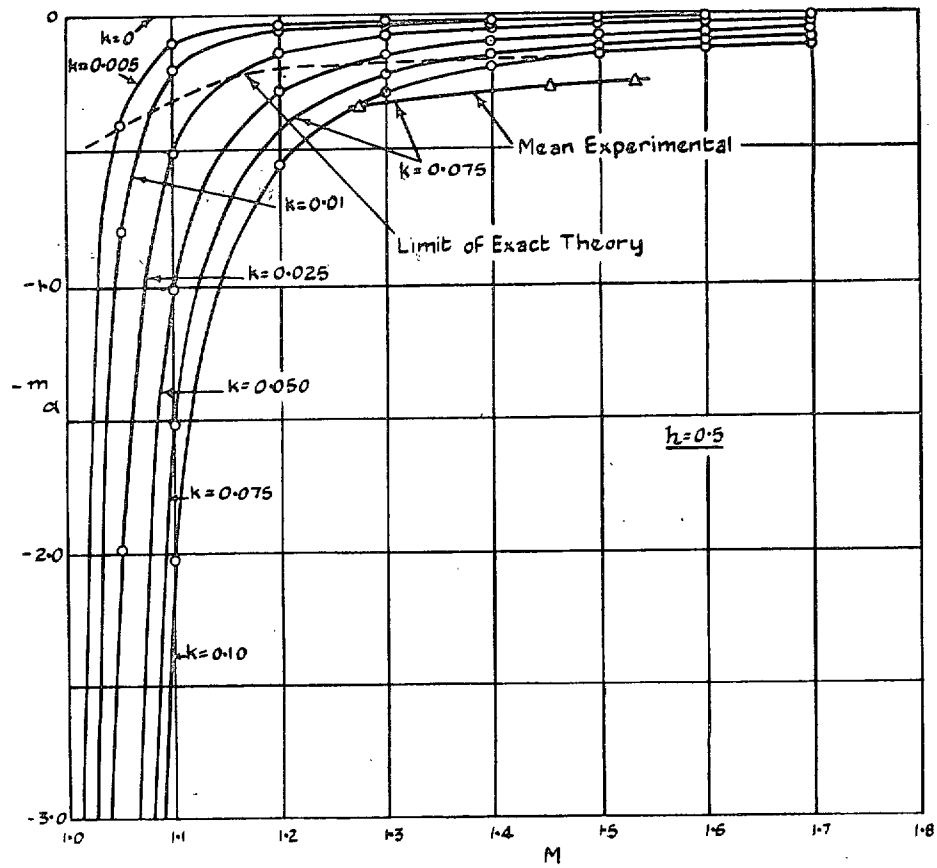


FIG. 6. Influence of thickness/chord ratio on the torsional aerodynamic stiffness coefficient.

Publications of the Aeronautical Research Council

ANNUAL TECHNICAL REPORTS OF THE AERONAUTICAL RESEARCH COUNCIL (BOUND VOLUMES)—

- 1936 Vol. I. Aerodynamics General, Performance, Airscrews, Flutter and Spinning. 40s. (41s. 1*d.*)
Vol. II. Stability and Control, Structures, Seaplanes, Engines, etc. 50s. (51s. 1*d.*)
- 1937 Vol. I. Aerodynamics General, Performance, Airscrews, Flutter and Spinning. 40s. (41s. 1*d.*)
Vol. II. Stability and Control, Structures, Seaplanes, Engines, etc. 60s. (61s. 1*d.*)
- 1938 Vol. I. Aerodynamics General, Performance, Airscrews. 50s. (51s. 1*d.*)
Vol. II. Stability and Control, Flutter, Structures, Seaplanes, Wind Tunnels, Materials. 30s. (31s. 1*d.*)
- 1939 Vol. I. Aerodynamics General, Performance, Airscrews, Engines. 50s. (51s. 1*d.*)
Vol. II. Stability and Control, Flutter and Vibration, Instruments, Structures, Seaplanes, etc. 63s. (64s. 2*d.*)
- 1940 Aero and Hydrodynamics, Aerofoils, Airscrews, Engines, Flutter, Icing, Stability and Control, Structures, and a miscellaneous section. 50s. (51s. 1*d.*)
- 1941 Aero and Hydrodynamics, Aerofoils, Airscrews, Engines, Flutter, Stability and Control, Structures. 63s. (64s. 2*d.*)
- 1942 Vol. I. Aero and Hydrodynamics, Aerofoils, Airscrews, Engines. 75s. (76s. 3*d.*)
Vol. II. Noise, Parachutes, Stability and Control, Structures, Vibration, Wind Tunnels. 47s. 6*d.* (48s. 7*d.*)
- 1943 Vol. I. Aerodynamics, Aerofoils, Airscrews. 80s. (81s. 4*d.*)
Vol. II. Engines, Flutter, Materials, Parachutes, Performance, Stability and Control, Structures. 90s. (91s. 6*d.*)
- 1944 Vol. I. Aero and Hydrodynamics, Aerofoils, Aircraft, Airscrews, Controls. 84s. (85s. 8*d.*)
Vol. II. Flutter and Vibration, Materials, Miscellaneous, Navigation, Parachutes, Performance, Plates and Panels, Stability, Structures, Test Equipment, Wind Tunnels. 84s. (85s. 8*d.*)

ANNUAL REPORTS OF THE AERONAUTICAL RESEARCH COUNCIL—

1933-34	1s. 6 <i>d.</i> (1s. 8 <i>d.</i>)	1937	2s. (2s. 2 <i>d.</i>)
1934-35	1s. 6 <i>d.</i> (1s. 8 <i>d.</i>)	1938	1s. 6 <i>d.</i> (1s. 8 <i>d.</i>)
April 1, 1935 to Dec. 31, 1936.	4s. (4s. 4 <i>d.</i>)	1939-48	3s. (3s. 2 <i>d.</i>)

INDEX TO ALL REPORTS AND MEMORANDA PUBLISHED IN THE ANNUAL TECHNICAL REPORTS, AND SEPARATELY—

April, 1950 R. & M. No. 2600. 2s. 6*d.* (2s. 7½*d.*)

AUTHOR INDEX TO ALL REPORTS AND MEMORANDA OF THE AERONAUTICAL RESEARCH COUNCIL—

1909-1949 R. & M. No. 2570. 15s. (15s. 3*d.*)

INDEXES TO THE TECHNICAL REPORTS OF THE AERONAUTICAL RESEARCH COUNCIL—

December 1, 1936 — June 30, 1939.	R. & M. No. 1850.	1s. 3 <i>d.</i> (1s. 4½ <i>d.</i>)
July 1, 1939 — June 30, 1945.	R. & M. No. 1950.	1s. (1s. 1½ <i>d.</i>)
July 1, 1945 — June 30, 1946.	R. & M. No. 2050.	1s. (1s. 1½ <i>d.</i>)
July 1, 1946 — December 31, 1946.	R. & M. No. 2150.	1s. 3 <i>d.</i> (1s. 4½ <i>d.</i>)
January 1, 1947 — June 30, 1947.	R. & M. No. 2250.	1s. 3 <i>d.</i> (1s. 4½ <i>d.</i>)
July, 1951.	R. & M. No. 2350.	1s. 9 <i>d.</i> (1s. 10½ <i>d.</i>)

Prices in brackets include postage.

Obtainable from

HER MAJESTY'S STATIONERY OFFICE

York House, Kingsway, London, W.C.2; 423 Oxford Street, London, W.1 (Post Orders: P.O. Box 569, London, S.E.1);
13a Castle Street, Edinburgh 2; 39 King Street, Manchester 2; 2 Edmund Street, Birmingham 3; 1 St. Andrew's
Crescent, Cardiff; Tower Lane, Bristol 1; 80 Chichester Street, Belfast, or through any bookseller.